Vibrational Spectroscopy of Biomembranes

Zachary D. Schultz[1] and Ira W. Levin[2]

[1]Department of Chemistry and Biochemistry, University of Notre Dame, Notre Dame, Indiana 46556; email: Schultz.41@nd.edu

[2]National Institute of Diabetes and Digestive and Kidney Diseases, National Institutes of Health, Bethesda, Maryland 20892; email: iwl@helix.nih.gov

Annu. Rev. Anal. Chem. 2011. 4:343–66

First published online as a Review in Advance on April 1, 2011

The *Annual Review of Analytical Chemistry* is online at anchem.annualreviews.org

This article's doi: 10.1146/annurev-anchem-061010-114048

1947-5438/11/0715-0343$20.00

Keywords

IR, Raman, lipid bilayer, protein

Abstract

Vibrational spectroscopy, commonly associated with IR absorption and Raman scattering, has provided a powerful approach for investigating interactions between biomolecules that make up cellular membranes. Because the IR and Raman signals arise from the intrinsic properties of these molecules, vibrational spectroscopy probes the delicate interactions that regulate biomembranes with minimal perturbation. Numerous innovative measurements, including nonlinear optical processes and confined bilayer assemblies, have provided new insights into membrane behavior. In this review, we highlight the use of vibrational spectroscopy to study lipid-lipid interactions. We also examine recent work in which vibrational measurements have been used to investigate the incorporation of peptides and proteins into lipid bilayers, and we discuss the interactions of small molecules and drugs with membrane structures. Emerging techniques and measurements on intact cellular membranes provide a prospective on the future of vibrational spectroscopic studies of biomembranes.

1. INTRODUCTION

Cellular membranes perform essential roles in nature, ranging from compartmentalization to cell signaling, trafficking, adhesion, and transport. The understanding of membrane formation and regulation has advanced considerably in recent years. Forty years ago, for example, Singer & Nicolson (1) first proposed a thermodynamics-based fluid mosaic model for cellular membranes in which amphipathic protein molecules either span a defined lipid bilayer or function as integral or peripheral bilayer components. The structural concept of membranes has evolved toward a model involving specific lipid-lipid and lipid-protein interactions that dynamically regulate various phenomena, including membrane signaling and trafficking (2). The complexity of intact membranes complicates their study; however, the current development and application of model systems have led to substantial progress in elucidating the properties of bilayer assemblies (3). In particular, vibrational spectroscopy has played a significant role in detecting and quantifying the molecular interactions that occur with the lipid bilayer. In this review, we focus on a collection of IR and Raman spectroscopic measurements that have furthered our molecular understanding of membrane architecture and activity.

The label-free benefits of vibrational spectroscopic techniques enable the observation of biomolecules with minimal perturbation to the membrane assembly. Both lipids and proteins possess various chemical functional groups that allow the monitoring of component interactions associated with membrane systems (e.g., **Figure 1**) (4). By using IR spectroscopy to monitor changes in the frequencies and widths of vibrational peaks assigned to either the protein or the lipids, investigators observed molecular alterations in a porin-containing bilayer that were attributed to lipid-protein interactions (4). Useful vibrational modes reflected, in general, chemical functional group stretching and bending motions. Additionally, hydrogen bonding and other interactions among lipids, proteins, and other membrane component molecules can be observed as broadening effects, peak frequency shifts, and splitting of spectral features. Common vibrational modes used in assessing biomembranes are tabulated in **Table 1**.

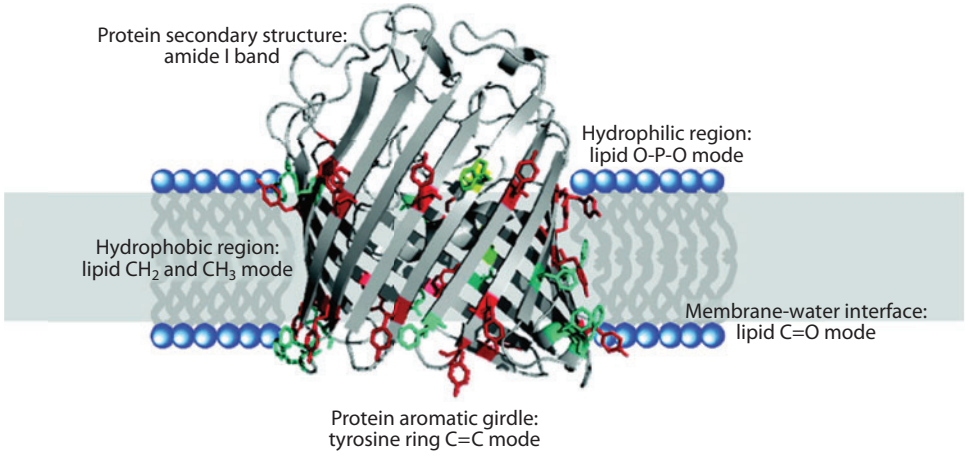

Figure 1

Illustration of a porin protein embedded in a lipid bilayer membrane, highlighting different functional groups that serve as vibrational spectroscopic reporters of the system. Both lipid and protein sections exhibit unique vibrational modes that enable the discrimination of chemical interactions in the membrane system. Figure taken from Reference 4.

Table 1 Common vibrational modes associated with lipids and proteins in biomembranes

Functional group mode	Approximate wave number (cm^{-1})
$-CH_3$, antisymmetric stretch	2,954
$-CH_3$, symmetric stretch	2,870
$-CH_2-$, antisymmetric stretch	2,924
$-CH_2-$, symmetric stretch	2,852
–S–H	2,570
–COH	883–873
–OH	1,097–1,086
$-CH_2-$, deformation	1,463–1,473
$-N^+(CH_3)_3$, symmetric stretch	722
$-N^+(CH_3)_3$, antisymmetric stretch	973
$-PO_2-$, symmetric stretch	1,084
$-PO_2-$, antisymmetric stretch	1,226
Amide I, α-helix	1,640–1,660
Amide I, β-sheet	1,630–1,640
Amide I, β-turn	1,670–1,690
Amide, random coil	1,640–1,650
Amide A, combination of amide II overtones with ν (–N–H)	3,250–3,300
Amide II, –N–H bend/C–N stretch	1,480–1,575
Amide III, –N–H bend/C–N stretch	1,230–1,330
Amide IV, deformation–O=C–N	625–770
Ring–C=C–phenylalanine	1,006
–C–C–	1,050–1,150
–C–O–	1,410
–C–S–, *gauche*	650
–C–S–, *trans*	700–745
–S–S–, disulfide conformation	510–540
Histidine imidazole mode	1,409
Tryptophan indole ring	880/1,361
Tyrosine doublet associated with ring modes	850/830
–C=O	1,734

In addition to chemical interactions, vibrational spectra are sensitive to membrane characteristics such as the lipid phases of the membrane bilayer and the orientation and conformation of bilayer constituents. In addition to the power and potential of vibrational spectroscopy, direct observation, at times aided by isotopic enrichment, of the vibrational features of specific moieties within a membrane system precludes the use of perturbing labels that are utilized, for example, in spectroscopic techniques such as fluorescence and electron paramagnetic resonance. Below, we discuss the use of specific vibrational modes that reflect lipid and protein moieties, both to determine membrane structure and composition and to monitor critical bilayer interactions.

An important aspect of vibrational spectroscopic studies has been the development of innovative vibrational spectroscopic measurements for providing new perspectives on the function of biological systems. For example, Fourier transform IR (FTIR) microspectroscopic imaging has demonstrated, with millisecond temporal resolution, the ability to monitor nonrepetitive reorganizational dynamics of aqueous dispersions of lipid vesicles (5). The spatially and temporally

FTIR: Fourier transform IR

ATR: attenuated total reflectance

DMPC: dimyristoylphosphatidylcholine

DPPC: dipalmitoylphosphatidylcholine

POPC: palmitoyl-oleoylphosphatidylcholine

SUV: small unilamellar vesicle

SERS: surface-enhanced Raman spectroscopy

HBM: hybrid bilayer membrane

IRRAS: IR reflection absorption spectroscopy

SFG: sum frequency generation

SFVS: sum frequency vibrational spectroscopy

CARS: coherent anti-Stokes Raman spectroscopy

resolved images allow direct and simultaneous determinations of various physical and chemical properties of multilamellar vesicles, including the main thermal gel–to–liquid-crystal phase transition, vesicle diffusion rates in both phases, and the variation in lipid bilayer–packing properties between the inner and outer lamellae that define the vesicle. Attenuated total reflectance (ATR) FTIR measurements yield an additional level of sensitivity. ATR-FTIR shows that polyethylene glycol–supported bilayers successfully reconstitute integral membrane proteins such that they exhibit physiological lateral diffusion properties (6). Notably, the polymer bands in these systems do not obscure lipid or protein bands, thereby facilitating protein secondary structure and lipid-protein-interaction analyses.

In addition to IR measurements, Raman spectroscopic methodologies have been creatively utilized in characterizing bilayer assemblies. Temperature- and polarization-dependent total internal reflection Raman spectroscopy was used to evaluate the properties of single lipid bilayers of dimyristoylphosphatidylcholine (DMPC), dipalmitoylphosphatidylcholine (DPPC), and palmitoyl-oleoylphosphatidylcholine (POPC) supported on glass (7). The formation of supported bilayers from DPPC-detergent mixtures monitored by TIR Raman spectroscopy demonstrated that the bilayers formed are free from detergent and that DPPC forms a gel-like bilayer identical to that obtained from the fusion of small unilamellar vesicles (SUVs) (8). Surface-enhanced Raman spectroscopic (SERS) measurements of lipid exchange from DMPC vesicles with perdeuterated DMPC hybrid bilayer membranes (HBMs) on gold nanoshells indicated that the lipids exchange with first-order kinetics at a rate of 1.3×10^{-4} s^{-1} (9). Substrates that exhibit nanostructure morphology, which enables SERS experiments, are simultaneously amenable to IR reflection absorption spectroscopy (IRRAS) techniques for characterizing membranes assembled on surfaces (10). Confocal Raman microscopy is capable of optically trapping liposomes to determine their molecular composition and unique interactions (11). The optical-trapping forces are sufficient to bend and alter the shape of a trapped vesicle while monitoring the intermolecular changes elicited by Raman scattering (12).

Nonlinear vibrational measurements such as sum frequency generation (SFG) [also referred to as sum frequency vibrational spectroscopy (SFVS)] and coherent anti-Stokes Raman spectroscopy (CARS) have also proven useful in unraveling aspects of membrane organization. SFG, a second-order nonlinear process, is highly sensitive to the symmetry and orientation of molecules. This orientational sensitivity has been used to study biomolecular configurations; the technique is also selective for interfaces, which allows monitoring of lipid bilayers (13–16). CARS using near-IR lasers tuned to specific vibrational modes has provided Raman spectroscopic measurements with a spatial resolution of several hundred nanometers (17). Multiplex CARS is also a powerful spectroscopic tool for monitoring spectral changes, such as those associated with lipid-phase transitions (18–20).

In the following sections, we review the use of vibrational spectroscopy to study lipid-lipid interactions and then examine recent work in which vibrational measurements have investigated the incorporation of peptides and proteins into lipid bilayers and the interactions between small molecules/drugs and membrane structures. Emerging techniques and measurements on intact cellular membranes provide a prospective on future vibrational spectroscopic studies on biomembranes.

2. LIPID BILAYER INTERACTIONS

2.1. Domain Organization

One of the most contentious topics surrounding biomembranes is the formation of putative membrane domains. The so-called lipid-raft hypothesis has spurred considerable interest in efforts to

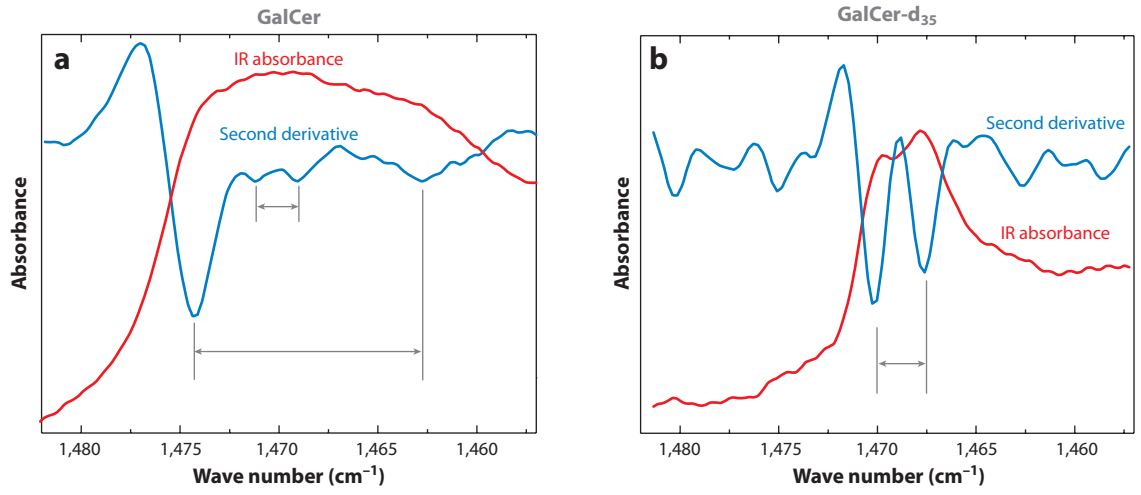

Figure 2

(*a*) Measurement of the correlation field splitting of the methylene-deformation mode of a galactocerebroside (GalCer) indicates a nanoscopic domain form within assemblies of GalCer, as well as in binary mixtures of GalCer and dipalmitoylphosphatidylcholine lipids. The measured IR absorbance is plotted in red, and the second derivative, used for peak detection, is plotted in blue. (*b*) Close inspection involving isotopic substitution indicates that phase-separation motifs result in partitioning of the sphingosine chain from the saturated fatty acid chain of GalCer lipids, which suggests the formation of microaggregate structures within the nanoscopic GalCer domains. Gray arrows denote the correlation field peak splittings that are used to determine domain size. Figure reproduced from Reference 21.

detect and elucidate the principles of domain formation. The elusive nature of such membrane complexes illustrates the necessity of using label-free techniques for detection. The presence of macroscopic phase-separated domains within model lipid membrane assemblies has been well established. Although phase-separated domains can be studied through various techniques, vibrational spectroscopy offers insights into the structure and dynamics associated with these transient phenomena.

Analysis of the correlation field splitting [i.e., observed splitting of methylene (CH_2) deformation modes arising from symmetry constraints in orthorhombically packed lipids] of lipid assemblies may be a useful method for detecting and characterizing nanoscale microdomain formation (21, 22). Splittings of the CH_2 deformation mode have been observed for galactocerebroside assemblies that correlate to clustering of either the sphingosine chain or the saturated acyl chain of the lipid (**Figure 2**). The identification of two separate splittings indicates the preferential clustering of lipid acyl chains within this bilayer assembly (21). The magnitude of the splitting can be used to quantify the number of acyl chains in the cluster.

By examining the CH_2 scissoring and rocking modes of the lipid acyl chains, investigators monitored demixing kinetics in a stratum corneum model system, which provided a physiologically relevant model of barrier-formation kinetics (22). Further examination of the lipid-chain CH_2 scissoring, rocking, and stretching modes of stratum corneum mixtures prepared with equimolar cholesterol and ceramide concentrations, in addition to variations in free fatty acid levels, showed that at lower free fatty acid content orthorhombic and hexagonal domains coexisted within the lipid lamellae. These results suggest that this configuration is present in skin at 32°C (23). The observed mode-splitting effects arise from nearest-neighbor interactions, which provide a quantitative measure of domain sizes. Clusters of three to five saturated acyl chains were reported in a model stratum corneum system (24). In this system, coupling of the sphingosine chains was not

observed, suggesting that these chains are physically isolated. In a separate study that examined interactions between cholesterol, galactocerebroside, and DPPC, the saturated acyl chains coupled preferentially; however, at sufficiently low temperatures, small splittings were observed for the sphingosine chains, indicating the formation of microenclosures within the sphingolipid domains (21).

DSPC: distearoylphosphatidylcholine

DPPS: dipalmitoylphosphatidylserine

Sterols play critical roles in the formation of membrane microdomains. Initial observations of detergent-resistant membrane fragments led to the formulation of the lipid raft concept. Interestingly, examination of the IR spectra obtained in these studies provides additional insight into the chemical interactions that control domain formation. A preferential interaction between cholesterol and galactocerebroside was observed in a ternary assembly that also contained DPPC (21). It is commonly thought that cholesterol favors saturated acyl chains; however, in the ternary system, a clear preference for the sphingolipid component, rather than DPPC, indicates that more sophisticated interactions are involved. IR measurements of POPC, cerebrosides, and cholesterol support the formation of domains in which cholesterol acts to promote concentration-dependent domains (25). A sphingolipid amide band was deconvoluted from overlapping spectral bands in ATR-FTIR spectra to address cholesterol- and phase-dependent changes in egg sphingomyelin lipid bilayers associated with hydrogen-bonding interactions (26). Notably, FTIR studies demonstrated that lanosterol incorporation produces a less tightly packed bilayer than does cholesterol, as evidenced by increased hydration in the glycerol backbone region of the DPPC bilayer (27). This finding suggests that lanosterol is less miscible in DPPC bilayers than is cholesterol but that it perturbs the bilayers' organization to a greater extent, probably because of (*a*) the conformationally ruffled faces and larger cross-sectional area of the lanosterol molecule and (*b*) disrupted hydrogen bonding with adjacent DPPC molecules (27).

Phase separation drives the formation of large lipidic phases in model membranes. Micrometer-sized, phase-separated domains have been imaged using Raman microspectroscopy. In a study by Percot & Lafleur (28), regions enriched in cholesterol, palmitic acid, and ceramides (a common model for the stratum corneum) were mapped on the basis of distinct vibrational modes of the components. Further studies examining the interactions of domains to the addition of Ca^{2+} and cholesterol sulfate illustrated the effect of small molecules on lipid-mixing behavior. In a ceramide–cholesterol–palmitic acid system, chain heterogeneity had more dominant effects on lipid miscibility than on hydrophobic matching parameters (30).

SFG was recently used to examine the phase-separation motifs associated with cholesterol in planar lipid bilayer models. Levy & Briggman (31) studied temperature-dependent phase transitions as a function of cholesterol concentration and observed a cooperative unit size that suggested the formation of small (<10-nm) clusters. Liu & Conboy (32) later used the symmetry sensitivity of SFG to demonstrate that phase separation in a distearoylphosphatidylcholine (DSPC)-cholesterol mixture was a leaflet-dependent phenomenon. Further SFG studies indicate that small amounts of cholesterol induce a disproportionately large increase in lipid order, which implies a molecular-level condensation effect (33).

A study examining the role of Mg^{2+} on the fusogenic properties of SUVs found that the binding of Mg^{2+} altered domain formation (34). IR measurements of DPPC-dipalmitoylphosphatidylserine (DPPS) mixtures indicated nonideal mixing; however, in the presence of Mg^{2+}, uniform correlation field splittings were observed, indicating that clusters of uniform size exist for various binary DPPC-DPPS composition ratios. In the presence of Mg^{2+}, a lateral binding interaction maintained a gel-phase packing configuration at elevated temperatures. This change was correlated to hypotheses regarding membrane tension for fusion. Examination of the IR spectra of DPPC-DPPS assemblies further indicated that Mg^{2+} is bound in the interfacial region of the bilayer without evidence of perturbation to the lipid head groups. Other IR studies

of DMPC and dimyristoylphosphatidylglycerol (DMPG) mixtures also demonstrated nonideal lipid mixing (35), illustrating a potential biological motif involving anionic lipids.

Laser scanning CARS microscopy was used to image coexisting domains within dioleoylphosphatidylcholine (DOPC)/DPPC-d_{62} (1:1)–supported bilayers incorporating 0–40% cholesterol on the basis of a model that derives the relative molecular concentration from the difference of the two intensities measured at the peak and dip frequencies of a CARS vibrational band (36). The limit of detection in CARS imaging is sufficient to detect phase separation in SUVs (37). Spectroscopic analysis of lipid vesicles using ultrabroadband CARS has also successfully monitored lipid vesicles (18). CARS measurements of lipid-chain CH_2 stretching modes have been correlated with differences between the packing densities of lipids in different thermodynamic phases, which suggests a means to detect phase separation in vivo (17).

DMPG: dimyristoylphosphatidylglycerol

DOPC: dioleoylphosphatidylcholine

TMCL: tetramyristoyl cardiolipin

2.2. Phase Transitions

Vibrational spectroscopy performed via the Kirchhoff-Levin two-state model has been used to monitor molecular interactions associated with thermodynamic phase transitions (38). Recent measurements have focused on unique bilayer molecules, interactions between molecules, and innovative methods for monitoring vibrations that can be associated with thermodynamic phase transitions. In studies examining Mg^{2+}-induced domain formation (described above), the curves measuring the transition from the gel phase to the liquid-crystal phase showed that the DPPC domains and the DPPS domains exhibit distinct phase transitions (**Figure 3**). This observation further supports the hypothesis that small lipid aggregates interact within the membrane assembly. In correlations with light scattering and fluorescence measurements, these domains have been postulated to explain the origins of the bilayer tension that promotes lipid bilayer fusion (34).

Raman measurements of C–C lipid-chain vibrations (1,050–1,150 cm^{-1}) in DPPC model membranes demonstrate that the dynamical transition at 200 K is accompanied by changes in lipid acyl–chain conformations in which the portion of the all-*trans* conformation decreases above the dynamical transition temperature (39). Two synthetic PEGylated lipids (where PEG refers to polyethylene glycol), 1,2-dimyristoyl-rac-glycerol-3-dodecaethylene glycol and 1,2-distearoyl-rac-glycerol-3-triicosaethylene glycol, have multiple phase transitions at 5.2°C and 21.2°C according to Raman spectroscopy (40). In a stratum corneum model system, FT-Raman measurements indicated that the incorporation of long-chain ω-acylceramides alters the phase-transition behavior of the system (41). In a binary system of deuterated DPPC and sphingosine phosphate, IR measurements, by monitoring each component individually, demonstrated that molecular interactions between the head groups of sphingosine phosphate and DPPC lead to increased hydration of the carbonyl group and to stabilization of the lipid bilayer structure (42).

IR studies of quadruple-chain anionic tetramyristoyl cardiolipin (TMCL) demonstrated that molecular interactions associated with multiple liquid-crystal phase transitions occur in bilayer models (43). The FTIR data indicated that in the L-c' phase, TMCL molecules possess tilted all-*trans* hydrocarbon chains packed into an orthorhombic subcell, whereas in the L-β and L-α phases, the all-*trans* hydrocarbon chains possess rotational mobility and are packed into a hexagonal subcell. The spectroscopic results demonstrate that the four carbonyl groups of the TMCL molecule become progressively more hydrated as one proceeds from the L-c' phase to the L-β phase, and then to the L-α phase; however, the head group phosphate moieties are hydrated in all three phases.

Cholesterol and other sterol molecules continue to show interesting phase transition–related interactions. Raman spectra of binary DPPC-cholesterol bilayers show little variation associated with cholesterol, which allows spectral changes to be assigned to the lipid-chain vibrational

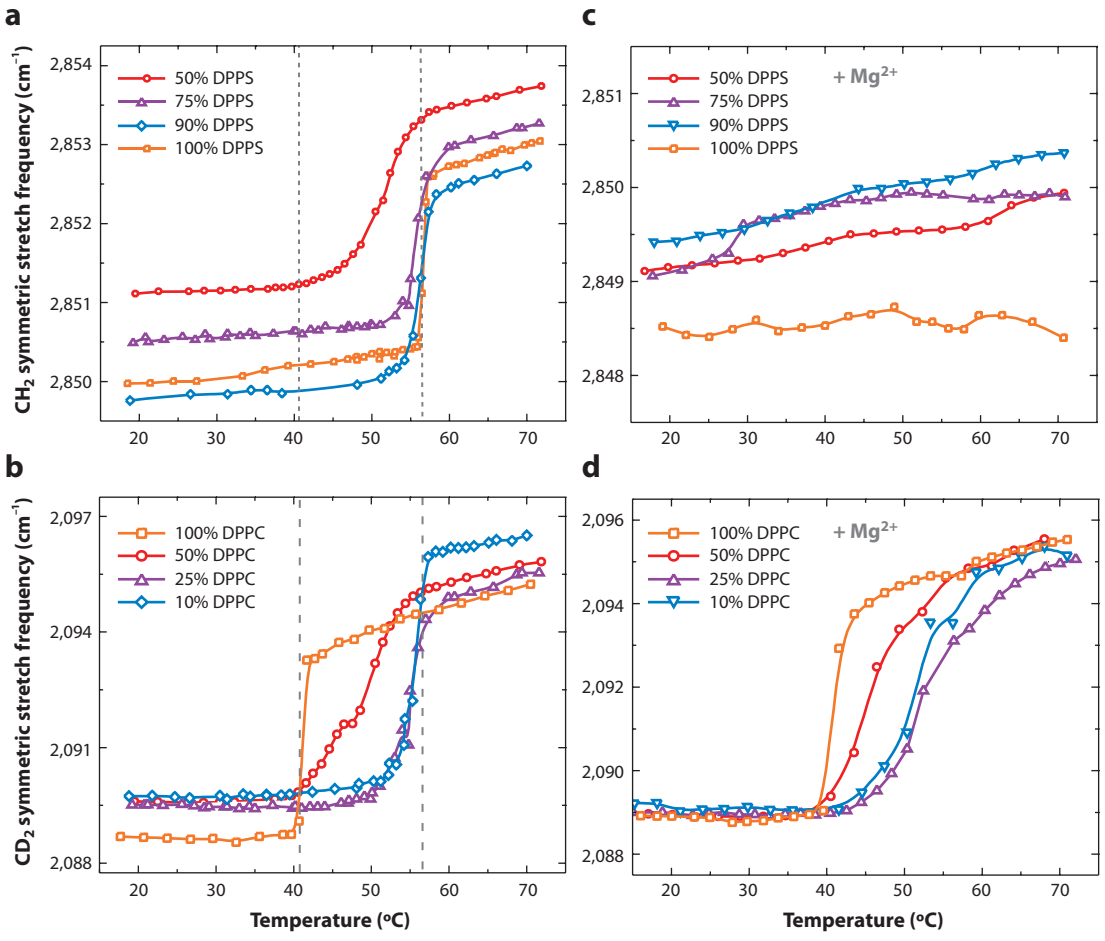

Figure 3

Curves measuring the transition from the gel phase to the liquid-crystal phase for binary assemblies of (*a*) dipalmitoylphosphatidylserine (DPPS) and (*b*) perdeuterated dipalmitoylphosphatidylcholine (DPPC-d_{62}), as well as with (*c*,*d*) Mg^{2+} added to the system. These curves allow one to draw conclusions about the mixing of the lipid components within the membrane assembly. Modified from Reference 34.

signatures of the liquid-disordered (l-d), solid-ordered (s-o), and liquid-ordered (l-o) phases (44). In saturated-chain phosphatidylglycerol (PG) lipid bilayers, cholesterol inclusion above 50% destroys cooperative phase transitions without the formation of cholesterol crystallites. Monitoring of C–H stretching, C=O stretching, and CH_2 bending modes revealed that cholesterol is immiscible with gel-phase PG lamellar layers (45). Ergosterol, which is structurally similar to cholesterol, appeared more effective for lowering the pretransition of DPPC bilayers, but it never achieved the level of anticooperativity associated with cholesterol in bilayers (46). In a binary mixture of DPPC and ergosterol (78:22 mol%), an l-o + s-o two-phase coexistence region existed up to 41°C, followed by an l-d + l-o coexistence region up to 57.5°C that yielded to an all-fluid-like l-d phase at higher temperatures (47). Epicholesterol is less miscible than cholesterol in DPPC bilayers, but it perturbs bilayer organization at lower concentrations than does cholesterol (48).

PG: phosphatidylglycerol

Optical-trapping confocal Raman microscopy offers significant experimental advantages by reducing sample volumes and minimizing background signals from particle surroundings. Further, chemical composition and structural information can be obtained from optically trapped particles in aqueous solution without the need for molecular labeling or extensive sample preparation (49). In one study, trapped vesicles were used to study the effects of phase and domain boundaries on ion transfer across a membrane (50). Trapped DPPC vesicles analyzed via a multivariate analysis method termed self-modeling curve resolution showed subtle pre- and subtransitions in agreement with calorimetry; however, the Raman spectra allowed additional molecular conformational analyses to be associated with the transition (51).

DSPE: distearoylphosphatidylethanolamine

DPPG: dipalmitoylphosphatidylglycerol

Nonlinear vibrational spectroscopies are also useful for monitoring phase transitions. Multiplex CARS measurements on single lipid bilayers have detected changes in lipid-chain conformations associated with both liquid-crystal phase–supported and gel phase–supported lipid bilayers (19). The detection limits in these experiments allowed the use of deuterated lipids for differentiating specific leaflets in asymmetrical bilayers. Maximum entropy methods applied to CARS data identified phase transitions in vesicles (20). SFG measurements have also been used to monitor single–bilayer phase transitions. The sensitivity of SFG spectroscopy was used to monitor the phase transitions of the lipid monolayer in an HBM, which showed that the underlying self-assembled monolayer did indeed affect the phase-transition properties (52). Furthermore, the transition temperature of the lipid leaflet in an HBM can be controlled by the identity of the underlying layer, as has been assessed by SFG measurements on HBMs with different molecules forming the self-assembled monolayer leaflet (53).

2.3. Bilayer Asymmetry

Because intact bilayer membranes exist asymmetrically, there are significant questions about biomembrane behavior that involve the molecular interaction between the individual bilayer lipid leaflets. However, SFVS results indicate that both leaflets of a DSPC bilayer adsorbed to a solid support have identical structures, which suggests that Langmuir-Blodgett and Langmuir-Schaefer deposition produces symmetric or asymmetric lipid bilayers that are suitable models for biological membrane studies (54). SFVS has been used with some success to monitor the kinetics of lipid exchange (flip-flop) (*a*) between bilayer leaflets as a function of temperature in pure lipid membranes and (*b*) in binary DSPC-DSPE (distearoylphosphatidylethanolamine) mixtures (55, 56). The selection rules for SFVS associated with interfacial symmetry enable the direct measurement of flip-flop kinetics. Asymmetrical bilayers prepared by use of deuterium substitution for one leaflet allow strong SFVS signals to be observed from oriented protonated-chain methyl groups (**Figure 4**). As the lipids interconvert between leaflets, the orientation of the protonated and deuterated methyl groups becomes symmetrical, and the SFVS signal diminishes. The pressure at which DPPC leaflets are prepared—for example, 28 mN m^{-1} versus 42 mM m^{-1}—results in an order-of-magnitude decrease in flip-flop kinetics for the higher-pressure bilayer (57).

The flip-flop rate in DSPC membranes increased two- to tenfold in the presence of gramicidin, which suggests that the peptide plays a transmembrane role (58). Incorporation of 1% of the amphipathic peptide melittin into a DSPC bilayer lowered the free-energy barrier and promoted lipid flip-flop, whereas the change associated with the hydrophobic WALP (23) peptide had a less pronounced effect on translocation (59). In dipalmitoylphosphatidylglycerol (DPPG) model systems, the effect on melittin on lipid exchange was highly sensitive to the concentration of melittin, such that at various concentrations different mechanisms were implicated (60).

These temperature-dependent SFVS measurements provided a direct spectroscopic probe of the phase transition in supported bilayer systems and suggested that bilayer leaflets exhibit

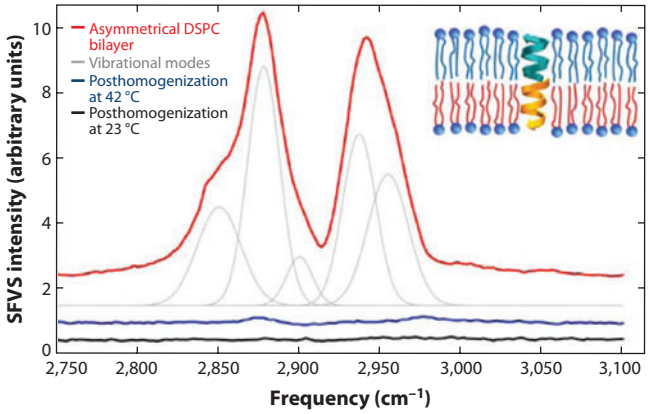

Figure 4

The sum frequency vibrational spectroscopy (SFVS) spectrum obtained from the methyl groups of an asymmetrical bilayer of protonated and perdeuterated distearoylphosphatidylcholine (DSPC) lipids (*red*). Through monitoring of the decrease of the SFVS signal intensity over time, the flip-flop kinetics can be determined. The SFVS signal after flip-flop homogenized the leaflets in experiments at 42°C (*blue*) and 23°C (*black*). The vibrational modes that fit to the observed spectrum are shown in gray. (*Inset*) Gramicidin inserted into an asymmetrical bilayer, where it reportedly increases the rate of flip-flop. Modified from Reference 58.

delocalized gel and liquid-crystal phase–domain structures (61). Cholesterol induced leaflet-specific domains in DSPC planar bilayers (32). Additionally, experiments involving selective deuteration permit orientation information to be determined from polarization-dependent measurements. SFVS measurements of DSPC bilayers determined that the acyl chains in both leaflets of supported bilayer membranes are oriented approximately 13° from the surface normal; however, there were differences between the orientation of the head groups in contact with the silica support (69° relative to normal) and the choline moiety in contact with the aqueous phase (66°) (54).

3. PEPTIDE-PROTEIN-DRUG INTERACTIONS

3.1. Peptides

Vibrational spectroscopy has been extensively used to characterize small-peptide conformations as models of the behavior of more complex proteins, particularly with respect to the conformational changes that occur in lipid bilayer environments. A 31-residue synthetic peptide, FP31, becomes more α-helical upon interacting with model membranes: Insertion increases the disorder of the liquid-crystal DPPC bilayer and dehydrates the polar regions surrounding the lipid carbonyls. However, in dielaidoyl phosphoethanolamine bilayers, FP31 destabilizes the bilayer and promotes the formation of a hexagonal phase (62). Polarization modulation (PM)-IRRAS and polarized ATR spectroscopy, coupled with Brewster angle microscopy and spectral simulations, were used to precisely determine the structure and the orientation of both the lipids in the bilayer and the FP23 peptide (the 23 N-terminal peptide of the human immunodeficiency virus gp41 protein) when the latter was inserted into the membrane (63). Wild-type α-synuclein unfolded in solution; however, the amide I mode converted into a β-sheet structure upon binding to PG membranes (64). Two-dimensional IR spectra in the amide I region for aggregates of the hexapeptide AcWL5 peptides with single isotopic labels indicated that AcWL5 forms membrane-bound aggregates dominated by a β-sheet secondary structure (65). IR measurements of the membrane-binding segment of hepatitis C virus also show changes in amide modes that depend on the composition of

PM: polarization modulation

the interacting bilayer (66). Polarized IR measurements indicated that the secondary structure and orientation of peptides believed to be the transmembrane domain of H^+-ATPase of *Saccharomyces cerevisiae* in lipid bilayer membranes are predominantly α-helical in DOPC membranes; however, the peptides self-assemble into oligomers of different sizes in which the helices express different tilt angles with respect to the surface normal (67).

DMPE: dimyristoylphosphatidylethanolamine

PC: phosphatidylcholine

An important class of peptides that has been studied by vibrational spectroscopy consists of antimicrobial peptides. IR measurements of surfactin demonstrate both dehydration of lipid carbonyls and increased fluidity, which may be important in the mechanism underlying the pore-forming antibiotic (68). IR was used to monitor both the transition from the gel phase to the liquid-crystal phase and the phosphate binding of magainin 2 in model systems (69). IR spectroscopy studies examining the secondary structure of distinctin, an antimicrobial peptide, showed that the membrane-bound peptide exhibited a less helical nature than did the peptide in solution (70). The antimicrobial peptides aurein 1.2, citropin 1.1, and maculatin 1.1, obtained from Australian tree frogs, adopted helical conformations upon interacting with model lipid bilayers of DMPC, DMPG, and dimyristoylphosphatidylethanolamine (DMPE). The effect to which the peptides altered the phase transitions of the bilayer varied with lipid and peptide identity (71). Melittin adsorption to DPPG altered the lipid layer structure, as observed in IR lipid spectra. Such lipid disruption was not observed for magainin and cecropin, the other antimicrobial peptides examined. In addition, melittin binding to the lipid bilayers occurred with 50% more frequency than did binding of either magainin or cecropin. Adsorption measurements obtained at the bare air-water interface indicated that surface activity followed the trend of melittin, magainin, and cecropin. IR amide spectra revealed that melittin adopts a helical structure only in the presence of lipid, whereas magainin and cecropin adopt helical conformations both in the presence of lipid and at the air-water interface (72). Plasticins derived from frog skin and analyzed by IR in DMPG (prokaryotic) and DMPC (eukaryotic) model systems showed that the most soluble cationic plasticins were strongly adsorbed, which induced noticeable perturbations to the bilayer acyl chains. This observation indicates possible insertion of these cationic plasticins into the bacterial membranes, whereas less-adsorbed cytotoxic, neutral plasticins resulted in membrane dehydration and the formation of peptide-membrane hydrogen bonds but caused little disturbance of lipid acyl chains at concentrations associated with antimicrobial activity (73). IR measurements of amphotericin B showed no changes in the order of the bilayer, but this compound is postulated to induce acyl-chain interdigitation of the lipid leaflets in association with its pore-forming properties (74). The mechanism of the bacteriocin lactocin 705 (Lac705), investigated through the use of DPPC vesicles, indicates that both the α- and β-subunits are required to kill cells. Further, where the Lac705 α component induces the dehydration of the bilayer interfacial region, the Lac705 β peptide inserts itself into the hydrophobic region of the membrane, establishing conditions for forming the transmembrane oligomer that can disrupt the lipid bilayer (75).

Additional studies have been performed examining the interactions between helical peptides and host membranes. IR spectra show conformational changes in alamethicin mutants where the methylalanine residues are converted to leucine. The amide I band indicates that the leucine substitutions induce stronger hydrogen bonding in the α-helical peptide, which is sensitive to membrane fluidity (76). Helical peptides alter transitions from the gel phase to the liquid-crystal phase in PG bilayer membranes to a greater extent than in phosphatidylcholine (PC) bilayers, which supports a role for hydrophobic mismatch in peptide-lipid interactions (77). The temperature at which the transition from the gel phase to the liquid-crystal phase occurs in the phosphatidylethanolamine bilayers is altered by these peptides in a hydrophobic mismatch–independent manner, in contrast to the hydrophobic mismatch–dependent manner observed with zwitterionic PC and anionic PG bilayers (78).

The combination of SFG and IR is a useful way to determine protein structure at interfaces (79). SFG and ATR showed that alamethicin, a model peptide for larger-channel proteins, adsorbs flat to gel phase–supported bilayers but is inserted and tilted in fluid-phase bilayers (13). The structure of β-sheets can also be determined with this methodology (14). Magainin 2 inserts itself into palmitoyl-oleoylphosphatidylglycerol (POPG) bilayers at a concentration of 800 nM, but it has been observed parallel to the bilayer both at lower concentrations and when interacting with a POPC bilayer (80). The interaction between melittin and a DPPG bilayer, as measured by an amide signal detected via SFG and IR and modeled against trial distributions, revealed two conformations for the peptide: one an ideal helix and the other a bent helix (15).

POPG: palmitoyl-oleoylphosphatidylglycerol

PLL: polylysine

Other peptide interactions alter lipid bilayer properties. The binding of polylysine (PLL) to DPPG-containing membranes increased the temperature of membrane-phase transitions but also caused phase separation of DPPG domains from other lipids, such as DPPC. The observed effects strongly depend on the length of the PLL. Further, PLL bound to model membranes in a helical structure (81). Polyamidoamine dendrimers were incorporated into DPPC model membranes at a rate of 3%, demonstrating strong interactions between polyamidoamine and the lipids that increased membrane fluidity, as measured by Raman scattering of the intensity ratios I-2,935/2,880; I-2,844/2,880; and I-1,090/1,130 of these respective vibrational frequencies (82). Compared with unsupported bilayers, confinement of lipid domains on porous substrates promoted the insertion of gramicidin S at temperatures below that of the transition from the gel phase to the liquid-crystal phase (83). Monitoring of the C=O stretching-mode vibrations allowed the formation of model membranes on agarose-coated silicon, which were electrochemically functional for gramicidin channels (84).

3.2. Proteins

Vibrational spectroscopy can assess the conformational properties of proteins and the lipid bilayer influence on the integrity and function of these proteins. For example, the bandwidths and frequencies of methyl and CH_2 stretching modes, carbonyl stretching modes, phosphate stretching modes, protein amide I modes, and the tyrosine sp2 C bond were used as reporter groups to examine the interactions between the lipid bilayer and different parts of a pore protein in a lipid bilayer (**Figure 1**) (4).

Numerous proteins undergo structural changes upon interacting with lipid bilayers; that is, the specific composition of the bilayer often affects the proteins' behavior. Examination of the half-width of the helical amide I mode of bacteriorhodopsin, extracted from purple membranes and reconstituted into a model membrane, demonstrated a lipid dependency on the conformational mobility of the protein (85). The band half-width correlated with the ability of the protein to undergo conformational change. Changes in bilayer thickness associated with DMPC or DSPC in the liquid-crystal phase have an impact on protein conformation mobility (**Figure 5**). The effect of the lipid environment on proteins is critical to understanding cellular processes at membrane interfaces.

In addition to modulating conformational changes, the hydrophobic environment of the bilayer interior can induce changes in protein structure. The secondary structure of lipid-modified RAS proteins interacting with in vitro membranes was assessed by ATR-IR spectroscopy (86). IR spectra indicate that bovine β-lactoglobulin converts to an α-helical structure upon binding with anionic lipids but that zwitterionic lipids do not alter its conformation. The degree of conversion depends on the lipid concentration and is strongly associated with the charge of the protein and lipids, as well as with the ionic strength of the solution (87). ATP-binding cassette transporters orient differently in DPPE (dipalmitoylphosphatidylethanolamine) bilayers than in DPPC (88).

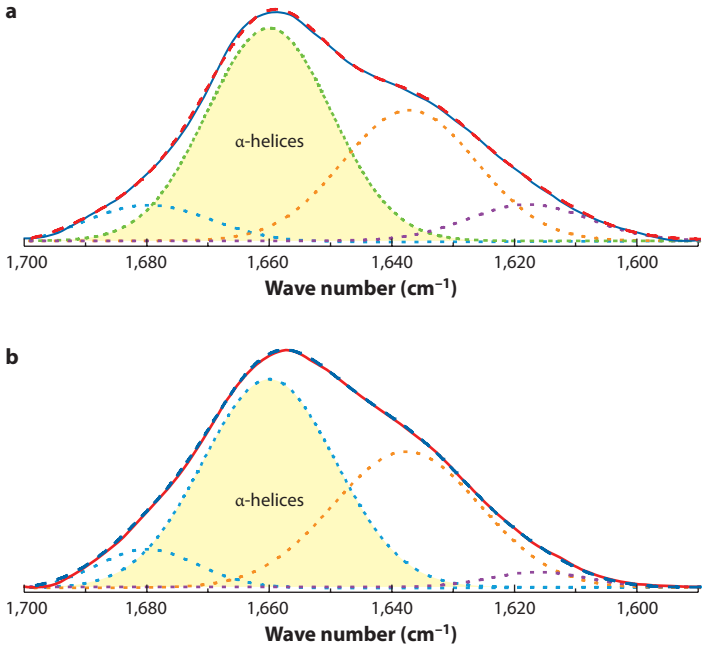

Figure 5

The full-width at half-maximum (FWHM) for the amide I region of bacteriorhodopsin (BR) in (*a*) a dimyristoylphosphatidylcholine (DMPC) bilayer and (*b*) a distearoylphosphatidylcholine (DSPC) bilayer. The FWHMs of the α-helical component of BR were 23.4 and 25.8 cm^{-1} for the DMPC and DSPC assemblies, respectively. The Fourier transform IR measurements were obtained at 60°C, at which both lipid assemblies are in the liquid-crystal phase, indicating that the lipid has an influence on protein mobility.

The conformation of bacterial proteins has been studied by IR spectroscopy. ATR-FTIR was used to determine the structure of FomA, a major outer-membrane protein of *Fusobacterium nucleatum*, in saturated-chain PC membranes (89). IR spectroscopic measurements of the secondary structure and local changes in the tyrosine microenvironment indicated that a mixed lipid system optimized the thermal stability of porin, perhaps by more adequately mimicking the diverse compositions in the outer membrane of the bacteria (90). Bacterial heat shock proteins showed evidence of lipid-protein interactions mediated by lipid head groups, and interactions between the protein and the bilayer's hydrophobic core stabilized model membranes (91). Measurement of the CH_2 stretching modes demonstrated interactions between (*a*) oxidized (ubiquinone 10) as well as reduced (ubiquinol 10) coenzyme Q_{10} and (*b*) DMPC, which suggests that the gel phase is more disordered in the presence of ubiquinol 10 versus ubiquinone 10. However, little effect was observed at liquid-crystal temperatures (92).

The nicotinic acetylcholine receptor interacts with both the hydrophobic core of the bilayer and charged groups on the surface of the bilayer. The α-helical amide I band at 1,655 cm^{-1} suffered no effect from long-term deuterium exchange, suggesting that these helices are buried in the hydrophobic core and are tilted at 40° in relation to the bilayer normal (93). Further studies showed that the acetylcholine receptor is stabilized by cations on the surface of the membranes (94). Monitoring of the amide modes of the nicotinic acetylcholine receptor in model membranes showed that anionic lipids affect the receptor's ability to change from a resting state to a desensitized state when challenged with an agonist (95). Examination of nicotinic acetylcholine receptors in different lipid bilayers indicated that the lipid matrix altered the receptor's response to the drug tetracaine (96).

The kinetics of the phospholipase enzyme PLA2, commonly derived from cobra venom, has been studied by numerous groups. IR analysis of the CH_3 group reveals an enantiomeric dependency on PLA2 action and, through the use of DPPC-supported bilayers in mechanistic studies, supports the so-called lag-burst hypothesis (97). PM-IRRAS studies showed that PLA2 activation depends on surface pressure; the pressure difference at liquid–liquid phase boundaries (domains) is sufficient to activate the enzyme (98). Investigators used optically trapped DMPC vesicles to monitor the kinetics of PLA2 by measuring changes in the lipid acyl–chain C–C *trans* and *gauche* isoforms and by correlating them to the extent to which PLA2 induced hydrolysis (99). This optical-trapping experiment required only two PLA2 enzymes on a single vesicle for detection.

Membrane fusion proteins, such as the SNARE proteins VAMP/synaptobrevin and syntaxin 1, convert into β-sheets related to the lipid–to–protein ratio content and to the lipid identity of the membrane (100). Vibrational spectroscopy indicates that membrane-bound v-SNAREs (VAMP2 and synaptobrevin2) are unstructured and that membrane-bound t-SNAREs (syntaxin and 1A/SNAP-25) are predominantly α-helical. v-SNAREs, but not t-SNAREs, exchange readily between the polymer-supported bilayer and lipid vesicles in solution, which suggests that v-SNAREs lack a transmembrane anchor (6).

Lipid bilayer–protein interactions have also been studied spectroscopically in photosynthetic membranes. An ATR-FTIR study revealed the secondary structure of the protein ferrodoxin in a bilayer composed of the chloroplast lipids monogalactosyldiacylglycerol and digalactosyldiacylglycerol: The structure was significantly altered by lipids and pH. However, the stabilization of ferrodoxin in the presence of lipids led to a greater rate of NADPH-dependent reduction of the dibromothymoquinone catalyzed by the enzyme (101). Cytochrome *c* was reconstituted into a lipid bilayer environment by detergent substitution, which was followed in situ by means of surface-enhanced IR absorption spectroscopy and normal-mode analyses (102). Through the use of a histidine tag, cytochrome *c* was incorporated into a model membrane on a gold surface (103). Cytochrome *c* can be oriented similar to its physiological conformation within a model bilayer membrane such that it becomes amenable to vibrational spectroscopic analysis (104). Oxygen reductase enzymes remained functional when the enzyme was reconstituted in a model membrane by use of surface vibrational spectroscopy (105). SERS has been successfully used to monitor cytochrome *c* immobilized and reconstituted in a membrane, which yielded new insights into proton translocation coupled to electron transfer in photosynthetic and mitochondrial systems (106).

The monitoring of membrane-protein interactions offers new routes to diagnostics and therapeutics. In addition to demonstrating that lipids act on proteins, SFG measurements have indicated that a signal protein, FGF-1, causes structural deformations in distearoylphosphatidylglycerol planar membranes. FGF-1, released as a function of cellular stress, was reversibly detected at a concentration of 1 nM by monitoring the lipid alkyl–chain deformations in a previously ordered bilayer (107). Potential cancer treatments involving antimicrobial peptides have been analyzed by ATR-FTIR to assess peptide conformation and bilayer disruption (108). Additionally, FTIR studies have established associations between oxidatively damaged lipid bilayers and the formation of Alzheimer's plaques (109). The secondary structure of human islet amyloid polypeptides expressed lipid composition–dependent aggregation on model membranes, including aggregation differences on membranes with model raft compositions that support seed-nucleated growth mechanisms for plaque formation (110).

3.3. Small Molecules and Drugs

In addition to studies that characterize interactions between peptides or proteins and lipid membranes, there are experiments that illustrate small-molecule and drug interactions with

membranes. For example, the carbonyl stretching–mode region of DPPC membranes changed when challenged with phytol and α-tocopherol, suggesting that these molecules associate at the interfacial regions of the membrane by forming hydrogen bonds but that they do not necessarily stabilize the membrane (111). The acyl chains of dipalmitoylphosphatidic acid (DPPA) monolayers and DPPA-POPC bilayers were affected when 2,4,5-trichlorophenol adsorbed to the model membranes, forming a heterodimer (112). Analysis of the CH_2 stretching, CH_2 scissoring, C=O stretching, and PO^{2-} stretching modes indicated that 3-pentadecylphenol orders the acyl chains in DPPC-liposome bilayers (113). PM-IRRAS measurements involving DMPC bilayers indicated that perfluorinated compounds increase bilayer fluidity and thickness by altering lipid-chain tilt in a manner reminiscent of cholesterol (114). Incorporating trehalose into phosphatidylethanolamine bilayers increases the conformational order of the hydrocarbon chains and dehydrates the interfacial region (115). Further, trehalose dehydrates phosphatidylserine head groups and alters the fluidity of dimyristoylphosphatidylserine bilayers (116). Binding of Ca^{2+} to POPG vesicles containing a human immunodeficiency virus fusion peptide caused the peptide to convert from an α-helix conformation to a β-sheet conformation, concomitant with the closure of the lytic pores (117).

DPPA: dipalmitoylphosphatidic acid

DMSO: dimethylsulfoxide

Numerous studies have examined the chemical alteration of the permeability of the stratum corneum. Combinations of chemicals affect skin permeability; for example, the combination of isopropyl myristate and glyceryl monocaprylate induces higher C–H stretching-mode frequencies of skin lipids than does isopropyl myristate alone (118). Dimethylsulfoxide (DMSO) partially disturbs lipid packing in a concentration-dependent fashion in model skin systems (119). SFG studies of DMSO on lipid monolayers assessed electrostatic head group interactions that affected the orientation and interaction of DMSO with the lipid leaflet (120). A combined IR and Raman study indicated that dipropylsulfoxide interacts with –CO, $–NH_3^+$, and $–PO_2^-$ groups in DMPE bilayers but only with $-N(CH_3)_3^+$ groups in membranes containing DMPC and DPPC (121). In another study of the stratum corneum, palmitic acid acted directly on acyl-chain organization and weakly interacted with polar head groups in the presence of keratin, which destabilized ceramide orthorhombic acyl-chain organization (122).

Interactions between membranes and specific drug molecules have also been examined. ATR-IR results showed that the chemotherapeutic drug dihydrochloride fluphenazine promotes fluidity in DPPC membranes prior to disrupting the bilayer at high concentrations (123). Pirarubicin, an anthracycline antibiotic, interacts preferentially with PG versus PC head groups when disrupting the bilayer (124). The antiviral drug arbidol preferentially interacts with anionic lipids to dehydrate the head groups of phospholipid membranes, which results in a solid-like phase configuration (125). Paclitaxel interacts with membranes, causing an increase in the asymmetric and symmetric CH_2 stretching modes, splitting of the CH_2 scissoring mode, and broadening of the carbonyl stretching modes. These findings suggest that this drug alters cooperativity and increases fluidity in the bilayer (126).

IR spectroscopy studies showed that arbutin, known to suppress melanin production in murine B16 melanoma cells and to inhibit phospholipase action, interacts with the hydrated populations of the carbonyl and phosphate groups by forming hydrogen bonds (127). SFG demonstrated that the orientation of an amphiphilic antibiotic molecule within a supported lipid bilayer is perpendicular to the membrane surface (128). The interaction between tricyclic antidepressants and lipid-phase transitions was studied by confocal Raman microscopy (129). IR investigations of the interaction between a prototype antineoplastic drug (paclitaxel) and a model DPPC cholesterol membrane suggested that cholesterol induces a condensing effect between paclitaxel and DPPC that restricts the penetration of the drug into the lipid leaflet (130). The nonsteroidal anti-inflammatory drug celecoxib decreases membrane fluidity and promotes phase separation at high concentrations

(131). HBMs formed onto gold nanoshells for SERS and surface-enhanced IR absorption spectroscopy measurements revealed that the overall hydrophobicity of ibuprofen is important for the intercalation of ibuprofen into the phospholipid leaflet in these membrane mimics (132). Optical-trapping confocal Raman microscopy of salicylate and ibuprofen interacting with DMPC vesicles demonstrated that although both drugs increase membrane disorder, only ibuprofen accumulates within the membrane (133).

4. FUTURE DIRECTIONS

The chemical specificity and label-free advantages of a plethora of vibrational spectroscopic techniques augur well for the continued use of the above-described approaches for investigating biomembrane behavior. Indeed, vibrational studies are now utilizing the many insights gained from bilayer studies of model systems to unravel the behavior of intact membrane assemblies. Numerous studies have investigated interactions that occur on skin, many of which verify properties observed in model systems, such as permeation and structural characteristics (134–139). Other applications of vibrational spectroscopy to intact membranes include (*a*) the examination of erythrocyte membrane hydration when treated with organic tin compounds (140), (*b*) the examination of toxicity effects of DMSO on the cellular membranes in human pulmonary endothelial cells (141), and (*c*) the monitoring of *Escherichia coli* viability associated with membrane hydration (142). ATR-IR spectroscopy has also demonstrated the incorporation of proteins into *E. coli* membranes (143). A topic that we expect to become more heavily investigated involves the detailed functional relationships between lipids and proteins in intact systems. For example, the fluidity of the native membrane environment of photoreceptor cells sensitively regulates conformational changes associated with the functions of the integral protein rhodopsin (144). Efforts to examine more sophisticated interactions between lipids and proteins have implicated PG lipids in the thylakoid membranes of tobacco plants as controlling chemical dynamics at the lipid-protein interface, as opposed to directly affecting protein secondary structure (145). Given the many emerging hypotheses and vast amounts of data regarding the critical roles of lipid domains (2), we expect new applications of detailed spectroscopic approaches to be developed and exploited.

To continue providing valuable information regarding critical interactions, particularly in intact membrane systems, vibrational spectroscopic measurements require constant innovation and renewal. Throughout this review, we describe results obtained from recently developed techniques, such as optical-trapping confocal Raman microspectroscopy; SFG; CARS; and other ingenious, cutting-edge strategies. An area that is poised to make an important contribution, particularly at the nanoscale level, is Raman enhancement from metal nanostructures that are traditionally associated with SERS. In one example involving an in vitro membrane, SERS-generated data from 100-nm silver colloidal particles were used to monitor the transport of Rhodamine 6G across a patch membrane under electrophysiological control; this detection strategy, however, is proposed to be more widely amenable to nonfluorescent molecules involving membrane transport (146).

In addition to providing increased sensitivity, nanoparticles offer a way to investigate membrane interactions on the length scales for which they are prepared. Preliminary results from tip-enhanced Raman spectroscopy studies suggest that this technique will become a robust tool for imaging membranes at the nanoscale (147–149). In one study, fluctuations in the Raman signal associated with the membrane of a fixed-rod photoreceptor cell were imaged with a spatial resolution of approximately 100 nm (**Figure 6**) (147). The examples of technological advances described herein indicate the potential of additional vibrational spectroscopic approaches to elucidate the intricate details of membrane behavior.

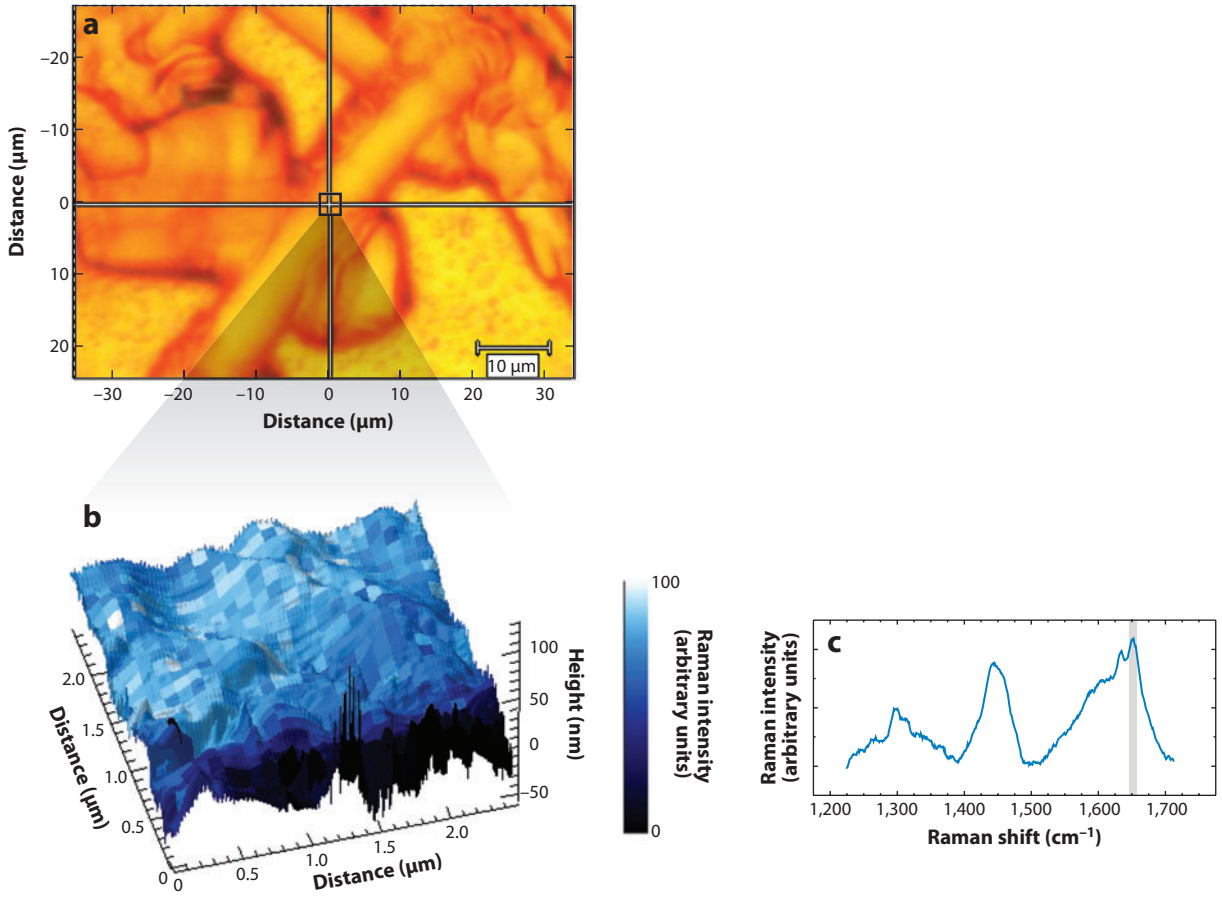

Figure 6

A tip-enhanced Raman spectroscopy map corresponding to the intensity of vibrational modes at 1,655 cm^{-1} in the measured spectrum (*c*), obtained from a 2,500 × 2,500 nm region of a fixed-rod photoreceptor cell (*a*). The topography (*b*) corresponds to the simultaneously obtained atomic force microscopy image. Image modified from Reference 147.

DISCLOSURE STATEMENT

The authors are not aware of any affiliations, memberships, funding, or financial holdings that might be perceived as affecting the objectivity of this review.

LITERATURE CITED

1. Singer SJ, Nicolson GL. 1972. The fluid mosaic model of the structure of cell membranes. *Science* 175:720–31
2. Lingwood D, Simons K. 2010. Lipid rafts as a membrane-organizing principle. *Science* 327:46–50
3. Chan Y-HM, Boxer SG. 2007. Model membrane systems and their applications. *Curr. Opin. Chem. Biol.* 11:581–87
4. Korkmaz F, Koster S, Yildiz O, Mantele W. 2008. The role of lipids for the functional integrity of porin: an FTIR study using lipid and protein reporter groups. *Biochemistry* 47:12126–34

5. Huffman SW, Schlucker S, Levin IW. 2004. Reorganizational dynamics of multilamellar lipid bilayer assemblies using continuously scanning Fourier transform infrared spectroscopic imaging. *Chem. Phys. Lipids* 130:167–74
6. Zhao J, Tamm LK. 2003. FTIR and fluorescence studies of interactions of synaptic fusion proteins in polymer-supported bilayers. *Langmuir* 19:1838–46
7. Lee CS, Bain CD. 2005. Raman spectra of planar supported lipid bilayers. *Biochim. Biophys. Acta Biomembr.* 1711:59–71
8. Lee C, Wacklin H, Bain CD. 2009. Changes in molecular composition and packing during lipid membrane reconstitution from phospholipid-surfactant micelles. *Soft Matter* 5:568–75
9. Kundu J, Levin CS, Halas NJ. 2009. Real-time monitoring of lipid transfer between vesicles and hybrid bilayer on Au nanoshells using surface enhanced Raman scattering (SERS). *Nanoscale* 1:114–17
10. Leverette CL, Dluhy RA. 2004. Vibrational characterization of a planar-supported model bilayer system utilizing surface-enhanced Raman scattering (SERS) and infrared reflection-absorption spectroscopy (IRRAS). *Colloids Surf. A* 243:157–67
11. Sanderson JM, Ward AD. 2004. Analysis of liposomal membrane composition using Raman tweezers. *Chem. Commun.* 2004:1120–21
12. Cherney DP, Bridges TE, Harris JM. 2004. Optical trapping of unilamellar phospholipid vesicles: investigation of the effect of optical forces on the lipid membrane shape by confocal-Raman microscopy. *Anal. Chem.* 76:4920–28
13. Ye SJ, Nguyen KT, Chen Z. 2010. Interactions of alamethicin with model cell membranes investigated using sum frequency generation vibrational spectroscopy in real time in situ. *J. Phys. Chem. B* 114:3334–40
14. Nguyen KT, King JT, Chen Z. 2010. Orientation determination of interfacial β-sheet structures in situ. *J. Phys. Chem. B* 114:8291–300
15. Chen XY, Wang J, Boughton AP, Kristalyn CB, Chen Z. 2007. Multiple orientation of melittin inside a single lipid bilayer determined by combined vibrational spectroscopic studies. *J. Am. Chem. Soc.* 129:1420–27
16. Chen XY, Wang J, Sniadecki JJ, Even MA, Chen Z. 2005. Probing α-helical and β-sheet structures of peptides at solid/liquid interfaces with SFG. *Langmuir* 21:2662–64
17. Li L, Cheng JX. 2008. Label-free coherent anti-Stokes Raman scattering imaging of coexisting lipid domains in single bilayers. *J. Phys. Chem. B* 112:1576–79
18. Kano H, Hamaguchi H. 2005. Ultrabroadband (>2500 cm^{-1}) multiplex coherent anti-Stokes Raman scattering microspectroscopy using a supercontinuum generated from a photonic crystal fiber. *Appl. Phys. Lett.* 86:121113
19. Wurpel GWH, Schins JM, Muller M. 2004. Direct measurement of chain order in single phospholipid mono- and bilayers with multiplex CARS. *J. Phys. Chem. B* 108:3400–3
20. Rinia HA, Bonn M, Muller M, Vartiainen EM. 2007. Quantitative CARS spectroscopy using the maximum entropy method: the main lipid phase transition. *ChemPhysChem* 8:279–87
21. Schultz ZD, Levin IW. 2008. Lipid microdomain formation: characterization by infrared spectroscopy and ultrasonic velocimetry. *Biophys. J.* 94:3104–14
22. Moore DJ, Snyder RG, Rerek ME, Mendelsohn R. 2006. Kinetics of membrane raft formation: fatty acid domains in stratum corneum lipid models. *J. Phys. Chem. B* 110:2378–86
23. Gooris GS, Bouwstra JA. 2007. Infrared spectroscopic study of stratum corneum model membranes prepared from human ceramides, cholesterol, and fatty acids. *Biophys. J.* 92:2785–95
24. Chen HC, Mendelsohn R, Rerek ME, Moore DJ. 2000. Fourier transform infrared spectroscopy and differential scanning calorimetry studies of fatty acid homogeneous ceramide 2. *Biochim. Biophys. Acta Biomembr.* 1468:293–303
25. Fidorra M, Heimburg T, Bagatolli LA. 2009. Direct visualization of the lateral structure of porcine brain cerebrosides/POPC mixtures in presence and absence of cholesterol. *Biophys. J.* 97:142–54
26. Arsov Z, Quaroni L. 2008. Detection of lipid phase coexistence and lipid interactions in sphingomyelin/cholesterol membranes by ATR-FTIR spectroscopy. *Biochim. Biophys. Acta Biomembr.* 1778:880–89

27. Mannock DA, Lewis R, McElhaney RN. 2006. Comparative calorimetric and spectroscopic studies of the effects of lanosterol and cholesterol on the thermotropic phase behavior and organization of dipalmitoylphosphatidylcholine bilayer membranes. *Biophys. J.* 91:3327–40
28. Percot A, Lafleur M. 2001. Direct observation of domains in model stratum corneum lipid mixtures by Raman microspectroscopy. *Biophys. J.* 81:2144–53
29. Arseneault M, Lafleur M. 2007. Cholesterol sulfate and Ca^{2+} modulate the mixing properties of lipids in stratum corneum model mixtures. *Biophys. J.* 92:99–114
30. Brief E, Kwak S, Cheng JTJ, Kitson N, Thewalt J, Lafleur M. 2009. Phase behavior of an equimolar mixture of *N*-palmitoyl-D-erythro-sphingosine, cholesterol, and palmitic acid, a mixture with optimized hydrophobic matching. *Langmuir* 25:7523–32
31. Levy D, Briggman KA. 2007. Cholesterol/phospholipid interactions in hybrid bilayer membranes. *Langmuir* 23:7155–61
32. Liu J, Conboy JC. 2009. Phase behavior of planar supported lipid membranes composed of cholesterol and 1,2-distearoyl-*sn*-glycerol-3-phosphocholine examined by sum-frequency vibrational spectroscopy. *Vib. Spectrosc.* 50:106–15
33. Bonn M, Roke S, Berg O, Juurlink LBF, Stamouli A, Muller M. 2004. A molecular view of cholesterol-induced condensation in a lipid monolayer. *J. Phys. Chem. B* 108:19083–85
34. Schultz ZD, Pazos IM, McNeil-Watson FK, Lewis EN, Levin IW. 2009. Magnesium-induced lipid bilayer microdomain reorganizations: implications for membrane fusion. *J. Phys. Chem. B* 113:9932–41
35. Lewis R, Zhang YP, McElhaney RN. 2005. Calorimetric and spectroscopic studies of the phase behavior and organization of lipid bilayer model membranes composed of binary mixtures of dimyristoylphosphatidylcholine and dimyristoylphosphatidylglycerol. *Biochim. Biophys. Acta Biomembr.* 1668:203–14
36. Li L, Wang HF, Cheng JX. 2005. Quantitative coherent anti-Stokes Raman scattering imaging of lipid distribution in coexisting domains. *Biophys. J.* 89:3480–90
37. Potma EO, Xie XS. 2005. Direct visualization of lipid phase segregation in single lipid bilayers with coherent anti-Stokes Raman scattering microscopy. *ChemPhysChem* 6:77–79
38. Kirchhoff WH, Levin IW. 1987. Description of the thermotropic behavior of membrane bilayers in terms of Raman spectral parameters—a 2-state model. *J. Res. Natl. Bur. Stand.* 92:113–28
39. Surovtsev NV, Dzuba SA. 2009. Conformational changes of lipids in bilayers at the dynamical transition near 200 K seen by Raman scattering. *J. Phys. Chem. B* 113:15558–62
40. Bista RK, Bruch RF, Covington AM, Sorger A, Gerstmann T, Otto A. 2008. Investigations of thermotropic phase behavior of newly developed synthetic PEGylated lipids using Raman spectromicroscopy. *Biopolymers* 89:1012–20
41. Kessner D, Brezesinski G, Funari SS, Dobner B, Neubert RHH. 2010. Impact of the long chain ω-acylceramides on the stratum corneum lipid nanostructure. Part 1: Thermotropic phase behaviour of CER[EOS] and CER[EOP] studied using X-ray powder diffraction and FT-Raman spectroscopy. *Chem. Phys. Lipids* 163:42–50
42. Garcia-Pacios M, Collado MI, Busto JV, Sot J, Alonso A, et al. 2009. Sphingosine-1-phosphate as an amphipathic metabolite: its properties in aqueous and membrane environments. *Biophys. J.* 97:1398–407
43. Lewis R, Zweytick D, Pabst G, Lohner K, McElhaney RN. 2007. Calorimetric, X-ray diffraction, and spectroscopic studies of the thermotropic phase behavior and organization of tetramyristoyl cardiolipin membranes. *Biophys. J.* 92:3166–77
44. de Lange MJL, Bonn M, Muller M. 2007. Direct measurement of phase coexistence in DPPC/cholesterol vesicles using Raman spectroscopy. *Chem. Phys. Lipids* 146:76–84
45. McMullen TPW, Lewis R, McElhaney RN. 2009. Calorimetric and spectroscopic studies of the effects of cholesterol on the thermotropic phase behavior and organization of a homologous series of linear saturated phosphatidylglycerol bilayer membranes. *Biochim. Biophys. Acta Biomembr.* 1788:345–57
46. Mannock DA, Lewis R, McElhaney RN. 2010. A calorimetric and spectroscopic comparison of the effects of ergosterol and cholesterol on the thermotropic phase behavior and organization of dipalmitoylphosphatidylcholine bilayer membranes. *Biochim. Biophys. Acta Biomembr.* 1798:376–88
47. Puehse M, Jeworrek C, Winter R. 2008. The temperature-pressure phase diagram of a DPPC-ergosterol fungal model membrane—a SAXS and FT-IR spectroscopy study. *Chem. Phys. Lipids* 152:57–63

48. Mannock DA, Lee MYT, Lewis R, McElhaney RN. 2008. Comparative calorimetric and spectroscopic studies of the effects of cholesterol and epicholesterol on the thermotropic phase behaviour of dipalmitoylphosphatidylcholine bilayer membranes. *Biochim. Biophys. Acta Biomembr.* 1778:2191–202
49. Fox CB, Myers GA, Harris JM. 2007. Temperature-controlled confocal Raman microscopy to detect phase transitions in phospholipid vesicles. *Appl. Spectrosc.* 61:465–69
50. Cherney DP, Conboy JC, Harris JM. 2003. Optical-trapping Raman microscopy detection of single unilamellar lipid vesicles. *Anal. Chem.* 75:6621–28
51. Fox CB, Uibel RH, Harris JM. 2007. Detecting phase transitions in phosphatidylcholine vesicles by Raman microscopy and self-modeling curve resolution. *J. Phys. Chem. B* 111:11428–36
52. Anderson NA, Richter LJ, Stephenson JC, Briggman KA. 2006. Determination of lipid phase transition temperatures in hybrid bilayer membranes. *Langmuir* 22:8333–36
53. Anderson NA, Richter LJ, Stephenson JC, Briggman KA. 2007. Characterization and control of lipid layer fluidity in hybrid bilayer membranes. *J. Am. Chem. Soc.* 129:2094–100
54. Liu J, Conboy JC. 2005. Structure of a gel phase lipid bilayer prepared by the Langmuir-Blodgett/Langmuir-Schaefer method characterized by sum-frequency vibrational spectroscopy. *Langmuir* 21:9091–97
55. Liu J, Conboy JC. 2004. Direct measurement of the transbilayer movement of phospholipids by sum-frequency vibrational spectroscopy. *J. Am. Chem. Soc.* 126:8376–77
56. Anglin TC, Conboy JC. 2009. Kinetics and thermodynamics of flip-flop in binary phospholipid membranes measured by sum-frequency vibrational spectroscopy. *Biochemistry* 48:10220–34
57. Anglin TC, Conboy JC. 2008. Lateral pressure dependence of the phospholipid transmembrane diffusion rate in planar-supported lipid bilayers. *Biophys. J.* 95:186–93
58. Anglin TC, Liu J, Conboy JC. 2007. Facile lipid flip-flop in a phospholipid bilayer induced by gramicidin A measured by sum-frequency vibrational spectroscopy. *Biophys. J.* 92:L1–3
59. Anglin TC, Brown KL, Conboy JC. 2009. Phospholipid flip-flop modulated by transmembrane peptides WALP and melittin. *J. Struct. Biol.* 168:37–52
60. Chen XY, Wang J, Kristalyn CB, Chen Z. 2007. Real-time structural investigation of a lipid bilayer during its interaction with melittin using sum frequency generation vibrational spectroscopy. *Biophys. J.* 93:866–75
61. Liu J, Conboy JC. 2007. Asymmetric distribution of lipids in a phase segregated phospholipid bilayer observed by sum-frequency vibrational spectroscopy. *J. Phys. Chem. C* 111:8988–99
62. Aranda FJ, Teruel JA, Ortiz A. 2003. Interaction of a synthetic peptide corresponding to the N-terminus of canine distemper virus fusion protein with phospholipid vesicles: a biophysical study. *Biochim. Biophys. Acta Biomembr.* 1618:51–58
63. Castano S, Desbat B. 2005. Structure and orientation study of fusion peptide FP23 of GP41 from HIV-1 alone or inserted into various lipid membrane models (mono-, bi- and multibilayers) by FT-IR spectroscopies and Brewster angle microscopy. *Biochim. Biophys. Acta Biomembr.* 1715:81–95
64. Ramakrishnan M, Jensen PH, Marsh D. 2006. Association of α-synuclein and mutants with lipid membranes: spin-label ESR and polarized IR. *Biochemistry* 45:3386–95
65. Londergan CH, Wang JP, Axelsen PH, Hochstrasser RM. 2006. Two-dimensional infrared spectroscopy displays signatures of structural ordering in peptide aggregates. *Biophys. J.* 90:4672–85
66. Perez-Berna AJ, Bernabeu A, Moreno MR, Guillen J, Villalain J. 2008. The pre-transmembrane region of the HCV E1 envelope glycoprotein: interaction with model membranes. *Biochim. Biophys. Acta Biomembr.* 1778:2069–80
67. Kota Z, Pali T, Dixon N, Kee TP, Harrison MA, et al. 2008. Incorporation of transmembrane peptides from the vacuolar H^+-ATPase in phospholipid membranes: spin-label electron paramagnetic resonance and polarized infrared spectroscopy. *Biochemistry* 47:3937–49
68. Carrillo C, Teruel JA, Aranda FJ, Ortiz A. 2003. Molecular mechanism of membrane permeabilization by the peptide antibiotic surfactin. *Biochim. Biophys. Acta Biomembr.* 1611:91–97
69. Fukuoka S, Howe J, Andra J, Gutsmann T, Rossle M, Brandenburg K. 2008. Physico-chemical and biophysical study of the interaction of hexa- and heptaacyl lipid A from *Erwinia carotovora* with magainin 2–derived antimicrobial peptides. *Biochim. Biophys. Acta Biomembr.* 1778:2051–57

70. Serra MD, Cirioni O, Vitale RM, Renzone G, Coraiola M, et al. 2008. Structural features of distinctin affecting peptide biological and biochemical properties. *Biochemistry* 47:7888–99
71. Seto GWJ, Marwaha S, Kobewka DM, Lewis R, Separovic F, McElhaney RN. 2007. Interactions of the Australian tree frog antimicrobial peptides aurein 1.2, citropin 1.1 and maculatin 1.1 with lipid model membranes: differential scanning calorimetric and Fourier transform infrared spectroscopic studies. *Biochim. Biophys. Acta Biomembr.* 1768:2787–800
72. Lad MD, Birembaut F, Clifton LA, Frazier RA, Webster JRP, Green RJ. 2007. Antimicrobial peptide-lipid binding interactions and binding selectivity. *Biophys. J.* 92:3575–86
73. El Amri C, Lacombe C, Zimmerman K, Ladram A, Amiche M, et al. 2006. The plasticins: membrane adsorption, lipid disorders, and biological activity. *Biochemistry* 45:14285–97
74. Nguyen TS, Weers PMM, Raussens V, Wang Z, Ren G, et al. 2008. Amphotericin B induces interdigitation of apolipoprotein stabilized nanodisk bilayers. *Biochim. Biophys. Acta Biomembr.* 1778:303–12
75. Castellano P, Vignolo G, Farias RN, Arrondo JL, Chehin R. 2007. Molecular view by Fourier transform infrared spectroscopy of the relationship between lactocin 705 and membranes: speculations on antimicrobial mechanism. *Appl. Environ. Microbiol.* 73:415–20
76. Haris PI, Molle G, Duclohier H. 2004. Conformational changes in alamethicin associated with substitution of its α-methylalanines with leucines: a FTIR spectroscopic analysis and correlation with channel kinetics. *Biophys. J.* 86:248–53
77. Liu F, Lewis R, Hodges RS, McElhaney RN. 2004. Effect of variations in the structure of a polyleucine-based α-helical transmembrane peptide on its interaction with phosphatidylglycerol bilayers. *Biochemistry* 43:3679–87
78. Liu F, Lewis R, Hodges RS, McElhaney RN. 2004. Effect of variations in the structure of a polyleucine-based α-helical transmembrane peptide on its interaction with phosphatidylethanolamine bilayers. *Biophys. J.* 87:2470–82
79. Wang J, Paszti Z, Clarke ML, Chen XY, Chen Z. 2007. Deduction of structural information of interfacial proteins by combined vibrational spectroscopic methods. *J. Phys. Chem. B* 111:6088–95
80. Nguyen KT, Le Clair SV, Ye SJ, Chen Z. 2009. Molecular interactions between magainin 2 and model membranes in situ. *J. Phys. Chem. B* 113:12358–63
81. Schwieger C, Blume A. 2007. Interaction of poly(L-lysines) with negatively charged membranes: an FT-IR and DSC study. *Eur. Biophys. J. Biophys. Lett.* 36:437–50
82. Gardikis K, Hatziantoniou S, Viras K, Wagner M, Demetzos C. 2006. A DSC and Raman spectroscopy study on the effect of PAMAM dendrimer on DPPC model lipid membranes. *Int. J. Pharm.* 318:118–23
83. Alaouie AM, Lewis R, McElhaney RN. 2007. Differential scanning calorimetry and Fourier transform infrared spectroscopic studies of phospholipid organization and lipid-peptide interactions in nanoporous substrate–supported lipid model membranes. *Langmuir* 23:7229–34
84. Hirano-Iwata A, Oshima A, Onodera K, Aoto K, Taira T, et al. 2009. Self-formation of bilayer lipid membranes on agarose-coated silicon surfaces studied by simultaneous electrophysiological and surface infrared spectroscopic measurements. *Appl. Phys. Lett.* 94:243906
85. Hendler RW, Barnett SM, Dracheva S, Bose S, Levin IW. 2003. Purple membrane lipid control of bacteriorhodopsin conformational flexibility and photocycle activity—an infrared spectroscopic study. *Eur. J. Biochem.* 270:1920–25
86. Guldenhaupt J, Adiguzel Y, Kuhlmann J, Waldmann H, Kotting C, Gerwert K. 2008. Secondary structure of lipidated Ras bound to a lipid bilayer. *FEBS J.* 275:5910–18
87. Zhang XQ, Keiderling TA. 2006. Lipid-induced conformational transitions of β-lactoglobulin. *Biochemistry* 45:8444–52
88. Gustot A, Smriti, Ruysschaert JM, Mchaourab H, Govaerts C. 2010. Lipid composition regulates the orientation of transmembrane helices in HorA, an ABC multidrug transporter. *J. Biol. Chem.* 285:14144–51
89. Anbazhagan V, Vijay N, Kleinschmidt JH, Marsh D. 2008. Protein-lipid interactions with *Fusobacterium nucleatum* major outer membrane protein FomA: spin-label EPR and polarized infrared spectroscopy. *Biochemistry* 47:8414–23

90. Sukumaran S, Hauser K, Rauscher A, Mantele W. 2005. Thermal stability of outer membrane protein porin from *Paraeoccus denitrificans*: FT-IR as a spectroscopic tool to study lipid-protein interaction. *FEBS Lett.* 579:2546–50
91. Tsvetkova NM, Horvath I, Torok Z, Wolkers WF, Balogi Z, et al. 2002. Small heat-shock proteins regulate membrane lipid polymorphism. *Proc. Natl. Acad. Sci. USA* 99:13504–9
92. Ausili A, Torrecillas A, Aranda F, de Godos A, Sanchez-Bautista S, et al. 2008. Redox state of coenzyme Q_{10} determines its membrane localization. *J. Phys. Chem. B* 112:12696–702
93. Hill DG, Baenziger JE. 2006. The net orientation of nicotinic receptor transmembrane α-helices in the resting and desensitized states. *Biophys. J.* 91:705–14
94. Sturgeon RM, Baenziger JE. 2010. Cations mediate interactions between the nicotinic acetylcholine receptor and anionic lipids. *Biophys. J.* 98:989–98
95. daCosta CJB, Medaglia SA, Lavigne N, Wang SZ, Carswell CL, Baenziger JE. 2009. Anionic lipids allosterically modulate multiple nicotinic acetylcholine receptor conformational equilibria. *J. Biol. Chem.* 284:33841–49
96. Baenziger JE, Ryan SE, Goodreid MM, Vuong NQ, Sturgeon RM, Dacosta CJB. 2008. Lipid composition alters drug action at the nicotinic acetylcholine receptor. *Mol. Pharmacol.* 73:880–90
97. Tong YJ, Li N, Liu HJ, Ge AL, Osawa M, Ye S. 2010. Mechanistic studies by sum-frequency generation spectroscopy: hydrolysis of a supported phospholipid bilayer by phospholipase A_2. *Angew. Chem. Int. Ed.* 49:2319–23
98. Wagner K, Desbat B, Brezesinski G. 2008. Liquid-liquid immiscibility in model membranes activates secretory phospholipase A_2. *Biochim. Biophys. Acta Biomembr.* 1778:166–74
99. Cherney DP, Myers GA, Horton RA, Harris JM. 2006. Optically trapping confocal Raman microscopy of individual lipid vesicles: kinetics of phospholipase A_2–catalyzed hydrolysis of phospholipids in the membrane bilayer. *Anal. Chem.* 78:6928–35
100. Yassine W, Taib N, Federman S, Milochau A, Castano S, et al. 2009. Reversible transition between α-helix and β-sheet conformation of a transmembrane domain. *Biochim. Biophys. Acta Biomembr.* 1788:1722–30
101. Grzyb J, Gagos M, Gruszecki WI, Bojko M, Strzalka K. 2008. Interaction of ferredoxin: $NADP^+$ oxidoreductase with model membranes. *Biochim. Biophys. Acta Biomembr.* 1778:133–42
102. Ataka K, Giess F, Knoll W, Naumann R, Haber-Pohlmeier S, et al. 2004. Oriented attachment and membrane reconstitution of His-tagged cytochrome *c* oxidase to a gold electrode: in situ monitoring by surface-enhanced infrared absorption spectroscopy. *J. Am. Chem. Soc.* 126:16199–206
103. Friedrich MG, Kirste VU, Zhu JP, Gennis RB, Knoll W, Naumann RLC. 2008. Activity of membrane proteins immobilized on surfaces as a function of packing density. *J. Phys. Chem. B* 112:3193–201
104. Ataka K, Richter B, Heberle J. 2006. Orientational control of the physiological reaction of cytochrome *c* oxidase tethered to a gold electrode. *J. Phys. Chem. B* 110:9339–47
105. Todorovic S, Verissimo A, Wisitruangsakul N, Zebger I, Hildebrandt P, et al. 2008. SERR-spectroelectrochemical study of a cbb_3 oxygen reductase in a biomimetic construct. *J. Phys. Chem. B* 112:16952–59
106. Friedrich MG, Robertson JWF, Walz D, Knoll W, Naumann RLC. 2008. Electronic wiring of a multi-redox site membrane protein in a biomimetic surface architecture. *Biophys. J.* 94:3698–705
107. Doyle AW, Fick J, Himmelhaus M, Eck W, Graziani I, et al. 2004. Protein deformation of lipid hybrid bilayer membranes studied by sum frequency generation vibrational spectroscopy. *Langmuir* 20:8961–65
108. Papo N, Shai Y. 2003. New lytic peptides based on the D,L-amphipathic helix motif preferentially kill tumor cells compared to normal cells. *Biochemistry* 42:9346–54
109. Koppaka V, Paul C, Murray IVJ, Axelsen PH. 2003. Early synergy between Aβ42 and oxidatively damaged membranes in promoting amyloid fibril formation by Aβ40. *J. Biol. Chem.* 278:36277–84
110. Jha S, Sellin D, Seidel R, Winter R. 2009. Amyloidogenic propensities and conformational properties of ProIAPP and IAPP in the presence of lipid bilayer membranes. *J. Mol. Biol.* 389:907–20
111. Picquart M, Lefevre T. 2003. Raman and Fourier transform infrared study of phytol effects on saturated and unsaturated lipid multibilayers. *J. Raman Spectrosc.* 34:4–12

112. Siam M, Reiter G, Hunziker R, Escher B, Karpfen A, et al. 2004. Evidence for heterodimers of 2,4,5-trichlorophenol on planer lipid layers. A FTIR-ATR investigation. *Biochim. Biophys. Acta Biomembr.* 1664:88–99
113. Cieslik-Boczula K, Koll A. 2009. The effect of 3-pentadecylphenol on DPPC bilayers ATR-IR and ^{31}P NMR studies. *Biophys. Chem.* 140:51–56
114. Matyszewska D, Leitch J, Bilewicz R, Lipkowski J. 2008. Polarization modulation infrared reflection-absorption spectroscopy studies of the influence of perfluorinated compounds on the properties of a model biological membrane. *Langmuir* 24:7408–12
115. Ortiz A, Teruel JA, Espuny MJ, Marques A, Manresa A, Aranda FJ. 2008. Interactions of a *Rhodococcus* sp. biosurfactant trehalose lipid with phosphatidylethanolamine membranes. *Biochim. Biophys. Acta Biomembr.* 1778:2806–13
116. Ortiz A, Teruel JA, Espuny MJ, Marques A, Manresa A, Aranda FJ. 2009. Interactions of a bacterial biosurfactant trehalose lipid with phosphatidylserine membranes. *Chem. Phys. Lipids* 158:46–53
117. Saez-Cirion A, Nieva JL. 2002. Conformational transitions of membrane-bound HIV-1 fusion peptide. *Biochim. Biophys. Acta Biomembr.* 1564:57–65
118. Furuishi T, Fukami T, Suzuki T, Takayama K, Tomono K. 2010. Synergistic effect of isopropyl myristate and glyceryl monocaprylate on the skin permeation of pentazocine. *Biol. Pharm. Bull.* 33:294–300
119. Kwak S, Lafleur M. 2009. Effect of dimethyl sulfoxide on the phase behavior of model stratum corneum lipid mixtures. *Chem. Phys. Lipids* 161:11–21
120. Chen XK, Allen HC. 2009. Interactions of dimethylsulfoxide with a dipalmitoylphosphatidylcholine monolayer studied by vibrational sum frequency generation. *J. Phys. Chem. A* 113:12655–62
121. Bonora S, Di Foggia M, Markarian SA, Tugnoli V. 2009. Vibrational and calorimetric study on the effect of di-*n*-propylsulfoxide (DPSO) on DMPC, DPPC and DMPE liposomes. *J. Mol. Struct.* 935:115–22
122. Corbe E, Laugel C, Yagoubi N, Baillet A. 2007. Role of ceramide structure and its microenvironment on the conformational order of model stratum corneum lipids mixtures: an approach by FTIR spectroscopy. *Chem. Phys. Lipids* 146:67–75
123. Cieslik-Boczula K, Szwed J, Jaszczyszyn A, Gasiorowski K, Koll A. 2009. Interactions of dihydrochloride fluphenazine with DPPC liposomes: ATR-IR and ^{31}P NMR studies. *J. Phys. Chem. B* 113:15495–502
124. Cong WJ, Liu QF, Liang QL, Wang YM, Luo GA. 2009. Investigation on the interactions between pirarubicin and phospholipids. *Biophys. Chem.* 143:154–60
125. Villalain J. 2010. Membranotropic effects of arbidol, a broad anti-viral molecule, on phospholipid model membranes. *J. Phys. Chem. B* 114:8544–54
126. Dhanikula AB, Panchagnula R. 2008. Fluorescence anisotropy, FT-IR spectroscopy and ^{31}P NMR studies on the interaction of paclitaxel with lipid bilayers. *Lipids* 43:569–79
127. Frias MA, Winik B, Franzoni AB, Levstein PR, Nicastro A, et al. 2008. Lysophosphatidylcholine-arbutin complexes form bilayer-like structures. *Biochim. Biophys. Acta Biomembr.* 1778:1259–66
128. Chen XY, Tang HZ, Even MA, Wang J, Tew GN, Chen Z. 2006. Observing a molecular knife at work. *J. Am. Chem. Soc.* 128:2711–14
129. Fox CB, Harris JM. 2010. Confocal Raman microscopy for simultaneous monitoring of partitioning and disordering of tricyclic antidepressants in phospholipid vesicle membranes. *J. Raman Spectrosc.* 41:498–507
130. Zhao LY, Feng SS. 2006. Effects of cholesterol component on molecular interactions between paclitaxel and phospholipid within the lipid monolayer at the air-water interface. *J. Colloid Interface Sci.* 300:314–26
131. Sade A, Banerjee S, Severcan F. 2010. Concentration-dependent differing actions of the nonsteroidal anti-inflammatory drug, celecoxib, in distearoyl phosphatidylcholine multilamellar vesicles. *J. Liposome Res.* 20:168–77
132. Levin CS, Kundu J, Janesko BG, Scuseria GE, Raphael RM, Halas NJ. 2008. Interactions of ibuprofen with hybrid lipid bilayers probed by complementary surface-enhanced vibrational spectroscopies. *J. Phys. Chem. B* 112:14168–75
133. Fox CB, Horton RA, Harris JM. 2006. Detection of drug-membrane interactions in individual phospholipid vesicles by confocal Raman microscopy. *Anal. Chem.* 78:4918–24
134. Azeem A, Ahmad FJ, Talegaonkar S. 2009. Exploration of skin permeation mechanism of frusemide with proniosomes. *Pharmazie* 64:735–40

135. Mendelsohn R, Flach CR, Moore DJ. 2006. Determination of molecular conformation and permeation in skin via IR spectroscopy, microscopy, and imaging. *Biochim. Biophys. Acta Biomembr.* 1758:923–33
136. Amin S, Kohli K, Khar RK, Mir SR, Pillai KK. 2008. Mechanism of in vitro percutaneous absorption enhancement of carvedilol by penetration enhancers. *Pharm. Dev. Technol.* 13:533–39
137. Egawa M, Tagami H. 2008. Comparison of the depth profiles of water and water-binding substances in the stratum corneum determined in vivo by Raman spectroscopy between the cheek and volar forearm skin: effects of age, seasonal changes and artificial forced hydration. *Br. J. Dermatol.* 158:251–60
138. Zhang GJ, Moore DJ, Flach CR, Mendelsohn R. 2007. Vibrational microscopy and imaging of skin: from single cells to intact tissue. *Anal. Bioanal. Chem.* 387:1591–99
139. Rodriguez G, Barbosa-Barros L, Rubio L, Cocera M, Diez A, et al. 2009. Conformational changes in stratum corneum lipids by effect of bicellular systems. *Langmuir* 25:10595–603
140. Zylka R, Kleszczynska H, Kupiec J, Bonarska-Kujawa D, Hladyszowski J, Przestalski S. 2009. Modifications of erythrocyte membrane hydration induced by organic tin compounds. *Cell Biol. Int.* 33:801–6
141. Spindler R, Wolkers WF, Glasmacher B. 2009. Effect of Me_2SO on membrane phase behavior and protein denaturation of human pulmonary endothelial cells studied by in situ FTIR spectroscopy. *J. Biomech. Eng.* 131:074517
142. Scherber CM, Schottel JL, Aksan A. 2009. Membrane phase behavior of *Escherichia coli* during desiccation, rehydration, and growth recovery. *Biochim. Biophys. Acta Biomembr.* 1788:2427–35
143. Dodd CE, Johnson BRG, Jeuken LJC, Bugg TDH, Bushby RJ, Evans SD. 2008. Native *E. coli* inner membrane incorporation in solid-supported lipid bilayer membranes. *Biointerphases* 3:FA59–67
144. Ludeke S, Mahalingam M, Vogel R. 2009. Rhodopsin activation switches in a native membrane environment. *Photochem. Photobiol.* 85:437–41
145. Szalontai B, Kota Z, Nonaka H, Murata N. 2003. Structural consequences of genetically engineered saturation of the fatty acids of phosphatidylglycerol in tobacco thylakoid membranes. An FTIR study. *Biochemistry* 42:4292–99
146. Nair CM, Sabna C, Murty K, Ramanan SV. 2005. Permeability of R6G across Cx43 hemichannels through a novel combination of patch clamp and surface enhanced Raman spectroscopy. *Pramana J. Phys.* 65:653–61
147. Schultz ZD, Stranick SJ, Levin IW. 2009. Advantages and artifacts of higher order modes in nanoparticle-enhanced backscattering Raman imaging. *Anal. Chem.* 81:9657–63
148. Schmid T, Messmer A, Yeo BS, Zhang WH, Zenobi R. 2008. Towards chemical analysis of nanostructures in biofilms II: tip-enhanced Raman spectroscopy of alginates. *Anal. Bioanal. Chem.* 391:1907–16
149. Neugebauer U, Rosch P, Schmitt M, Popp J, Julien C, et al. 2006. On the way to nanometer-sized information of the bacterial surface by tip-enhanced Raman spectroscopy. *ChemPhysChem* 7:1428–30

Annual Review of
Analytical Chemistry

Volume 4, 2011

Contents

Indexes

Errata

An online log of corrections to the *Annual Review of Analytical Chemistry* articles may be found at http://arjournals.annualreviews.org/errata/anchem